Influence of silicon nanocrystals on the performance of Yb3+/Er3+: Bi2O3-GeO2 pedestal waveguides for amplification at 1542 nm

Diego S. da Silva, Marcos I. Alayo, Luciana R. P Kassab, Thiago A. A. de Assumpção, Niklaus U. Wetter, et al.

Diego S. da Silva, Marcos I. Alayo, Luciana R. P Kassab, Thiago A. A. de Assumpção, Niklaus U. Wetter, Ernesto Jimenez-Villar, "Influence of silicon nanocrystals on the performance of Yb3+/Er3+: Bi2O3-GeO2 pedestal waveguides for amplification at 1542 nm," Proc. SPIE 10521, Synthesis and Photonics of Nanoscale Materials XV, 105210M (15 February 2018); doi: 10.1117/12.2291326

SPIE.

Event: SPIE LASE, 2018, San Francisco, California, United States

Influence of silicon nanocrystals on the performance of Yb^{3+}/Er^{3+}: Bi_2O_3-GeO_2 pedestal waveguides for amplification at 1542 nm

Diego S. da Silva[a], Marcos I. Alayo[b], Luciana R. P. Kassab[c], Thiago A. A. de Assumpção[b], Niklaus, U. Wetter*[a], Ernesto Jimenez-Villar[a],
[a]Centro de Lasers e Aplicações, Instituto de Pesquisas Energéticas e Nucleares – IPEN-CNEN/SP, Rua Prof. Lineu Prestes 2242, São Paulo, Brazil;
[b]Escola Politécnica, Universidade de São Paulo, 05508-970, São Paulo, Brazil;
[c]Faculdade de Tecnologia de São Paulo, CEETEPS/UNESP, 01124-060, São Paulo, Brazil.

ABSTRACT

This paper reports for, the first time, the influence of silicon nanocrystals on the photoluminescence and optical gain of Yb^{3+}/Er^{3+} codoped Bi_2O_3–GeO_2 waveguides for amplification at 1542 nm. Pedestal waveguides were fabricated by RF- sputtering followed by optical lithography and reactive ion etching. RF-sputtering followed by heat treatment produced silicon nanocrystals with average size of 8 nm and resulted in a photoluminescence enhancement of about 10 times for the 520 nm and 1530 nm emission bands. The resulting internal gain was 5.5 dB/cm at 1542 nm, which represents and enhancement of ~50%, demonstrating potential for applications in integrated optics.

Keywords: Waveguides, Optical amplifiers, Photoluminescence, Nanomaterials.

1. INTRODUCTION

Photoluminescence enhancement (PE) of rare earth doped materials containing metallic nanoparticles (NPs) has been reported for photonics applications[1-3], where the enhancement was attributed to two phenomena; the local field in the vicinity of the metallic nanoparticles and the energy transfer from the NPs to the rare earth ions[4]. Semiconductor nanocrystals (quantum dots) is an alternative for PE due to their absorption cross sections that are larger than cross sections of rare earth (RE) ions [1, 5]. Energy transfer is very efficient in this case if the size of the quantum dots permits their energy gap to match with the radiative transitions of the RE ions. Erbium doped optical amplifier (EDFAs) have renewed interest in Er^{3+} doped materials for the production of evermore efficient devices such as optical amplifiers and fiber networks used in the telecommunication window at 1.5μm. In the case of Er^{3+} PE, there are examples that include mostly silicate films and waveguide devices with silicon nanocrystals prepared by using different techniques such as ion implantation, lithography, chemical vapor deposition and sputtering techniques[5]. Improvements of waveguides amplifiers based on Er^{3+} doped silicate thin films with silicon nanocrystals were also reported[6].

New material research in applications that requires higher refractive index for more nonlinear response and higher index contrast is motivated especially by the development of waveguides amplifiers. Heavy metal oxide materials are a good alternative due to their larger linear refractive index (~2.0), high nonlinear response and smaller cutoff phonon energy (500-700 cm^{-1})[7, 8]. There is a lack of literature related to research on heavy metal oxide glasses incorporating silicon nanostructures in comparison to other materials such as silica glasses. PE in Er^{3+} doped germanate glasses (Bi_2O_3–GeO_2**)** due to the presence of silicon NPs with size larger than 10 nm has been demonstrated elsewhere[9]. Growth of ~200% at the wavelength of 545 nm and ~100% in Er^{3+} emission at 525 nm, 660 nm and 1530 nm has also been shown[9]. Photoluminescence quenching was observed for samples containing silicon nanocrystals, especially in the near infrared region. PE of ~300% in the presence of silicon nanocrystals was reported for tellurite glasses doped with Er^{3+}, in the visible and near infrared regions[10]. Increased optical gain of 7dB/cm at 1535 nm was demonstrated in an Er^{3+} doped silicon–rich, silicon-oxide waveguide amplifier containing Si NPs[6].

*nuwetter@ipen.br; phone +55 11 3133 9359; www.ipen.br

Synthesis and Photonics of Nanoscale Materials XV, edited by Jan J. Dubowski, Andrei V. Kabashin, Linyou Cao, David B. Geohegan, Proc. of SPIE Vol. 10521, 105210M · © 2018 SPIE
CCC code: 0277-786X/18/$18 · doi: 10.1117/12.2291326

These results motivated the present study that report for the first time the influence of Si nanocrystals in the photoluminescence of Yb^{3+}/Er^{3+} codoped Bi_2O_3 –GeO_2 (BGO) waveguides for amplification at 1542 nm. We demonstrate the possibility of producing Si nanocrystals using the sputtering technique followed by adequate heat treatment avoiding the use of more complex processes. As a result, we achieve an enhancement of approximately ten times at 520 nm and 1530 nm and a 50% increase of the optical gain of the waveguide at 1542 nm.

2. EXPERIMENTAL

P-type wafers with of 3.0 in diameter were used in conventional microelectronics fabrication techniques to produce the pedestal waveguides, following the sequence shown by Assumpção et al.[10]. The core of the waveguides, constituted of Yb^{3+}/Er^{3+} codoped BGO thin films with and without Si nanostructures, were produced using RF magnetron sputtering placing the RE pellets upon the BGO target in one of the electrodes of the system and the silicon target onto the other electrode. The BGO (wt%: 41.6 Bi_2O_3- 58.4 GeO_2) target and the RE pellets were produced by mixing the powders, submitting them to uniaxial pressure followed by sintering. A commercial Si target was used for the waveguides containing silicon nanostructures. The RF power at 13.56 MHz was set to 70 W for the electrode of the BGO target and to 9W for the silicon target (only for the production of the thin film containing the Si nanocrystals). The obtained waveguides were annealed at 440 °C during 3 hours to become transparent and also to nucleate Si nanostructures. Small angle X ray scattering (SAXS), Energy dispersive spectroscopy (EDS) and High resolution transmission electron microscopy (HR-TEM) were performed in order to obtain information about the structure and morphology of the silicon nanostructures. The concentration of the RE ions was determined by Rutherford backscattering spectrometry (RBS) and particle induced X-ray emission (PIXE) analysis. The pedestal profile was analyzed by Scanning Electron Microscopy (SEM). The RE concentrations in both samples, with and without Si nanostructures, were $[Er^{3+}]$ = 1.34E21 at/cm^3, $[Yb^{3+}]$ = 3.90E21 at/cm^3 and $[Er^{3+}]$ = 1.00E21 at/cm^3, $[Yb^{3+}]$ = 2.76E21 at/cm^3 respectively.
Propagation losses at 1068 nm (ytterbium fiber laser) were determined using the 'topview' technique[11]. In these measurements the edges of the silicon wafer were cleaved to acess the inputs and outputs of the waveguides, resulting in optical devices with a length of 1 cm. The near field profiles of the waveguides at 1068 nm were obtained using a CCD camera positioned in front of an objective lens (10x) placed in the output of the waveguide to determine the mode propagation for different waveguide widths. Simulated near-field profile patterns were also obtained by the finite difference time domain (FDTD) method using OptiFDTD software.

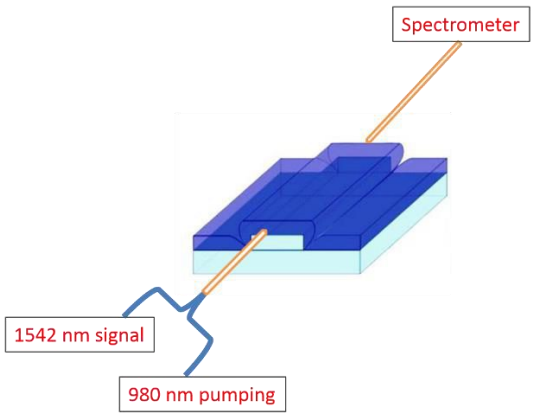

Figure 1. Illustration of the set-up for the gain measurement.

Infrared (IR) and infrared-to-visible upconversion photoluminescence spectra were obtained using a 980 nm cw diode laser for excitation. The detecting the light emitted from the surface of the waveguides was done with a monochromator, an optical detector (photomultiplier-tube and germanium-photodiode, for the visible and infrared regions, respectively) and a lock-in. The measurements confirmed the incorporation of RE ions in the trivalent form and that the Si nanostructures influence the $^4I_{13/2} \rightarrow {}^4I_{15/2}$ infrared emission of Er^{3+}.
The infrared gain at 1542 nm was measured using 980 nm and 1542 nm for pump and signal wavelengths, respectively (see figure 1). Both wavelengths are multiplexed inside a waveguide division multiplexer (WDM)

into the pedestal waveguides using single mode fibers. The signal power coupled to the waveguides was kept low to prevent gain saturation. The output signal was collected by an optical fiber and sent to an optical spectrum analyzer, in order to evaluate the gain with the setup described in figure 1. The value of the gain is given by the ratio of the signal peak with and without 980 nm pumping[12].

3. RESULTS AND DISCUSSIONS

The PL spectra of the Yb^{3+}/Er^{3+} codoped BGO pedestal waveguides with and without Si NPs, resulting in near infrared (NIR) to infrared frequency downconversion and NIR to visible upconversion, are shown in Figure 1 (980 nm excitation). An enhancement of the peak intensities of 7 and 10 times for λ=530 nm and λ=1530 nm, respectively, occurs in the presence of Si nanocrystals (see figure 2). The large PE (around ten times) at 1530 nm may be attributed to the contribution of Si nanocrystals. Also observed is the emission at 1200 nm from the Bi^{+} ions, which decreases in the presence of silicon nanocrystals. The insertion of Si followed by the formation into Si nanocrystals may reduce [Bi^{+}]; the [Bi^{+}] decrease may cause luminescence decrease at ~1200 nm. Clearly, an in depth study about this mechanism is required in order to confirm our hypothesis, but this issue is beyond the scope of this manuscript.

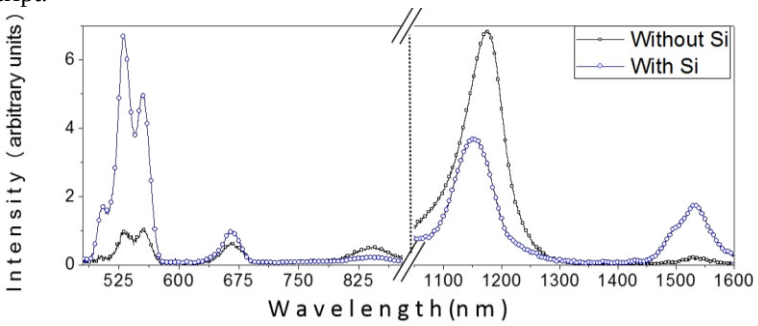

Figure 2. Photoluminescence spectra of Er^{3+}/Yb^{3+} codoped BGO thin films under excitation at 980 nm.

Very little difference (<6%) was observed in radiative lifetimes measurements. For the samples with and without Si nanocrystals, differences of 21.8 μs and 28.9 μs were obtained, respectively, for the photoluminescence band centered at 550 nm and 5.81 ms and 5.5 ms for the band at λ=1530 nm.

Figures 3a and 3b show the HR-TEM and electron diffraction pattern analysis of the Yb^{3+}/Er^{3+} codoped BGO pedestal waveguide, giving information about the size and cubic structure of the nanocrystals[13]. The EDS results, shown in Figure 3c, corroborate the presence of Si. Small angle x-ray scattering (SAXS) measurements were performed and the results were analyzed with the 'gnom' software.

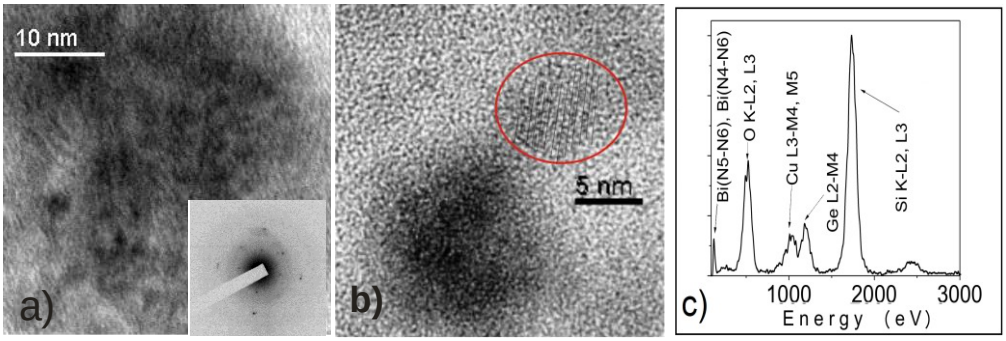

Figure 3. HR-TEM images of the thin film waveguide containing NPs. a) inset: image of electron diffraction pattern. b) Close-up showing an isolated NP (circle) and Si agglomerate (dark spot in lower part). c) Energy dispersive spectroscopy analysis of image 2b).

For this analysis, the information obtained with the HR-TEM measurements was used, since it is necessary to have an idea of the morphology of the particles in order to fit the scattering curve obtained from SAXS measurements. The results suggest a high density of crystals with diameter near 8 nm. The Si NP's filling fraction was estimated at 4.65%, which was determined considering the results obtained from RBS for the chemical composition, and the densities of the germanate host (6.2g/cm^3) and Si nanocrystals (2.3296 g/cm^3 for cubic structure).
The Er $^{3+}$/Yb^{3+} codoped BGO pedestal waveguide with a height of 510 nm, observed by scanning electron microscopy (SEM) in figure 4, promoted the smallest propagation loss in a group of samples with different thin film thickness, varying from 300 to 1000 nm.

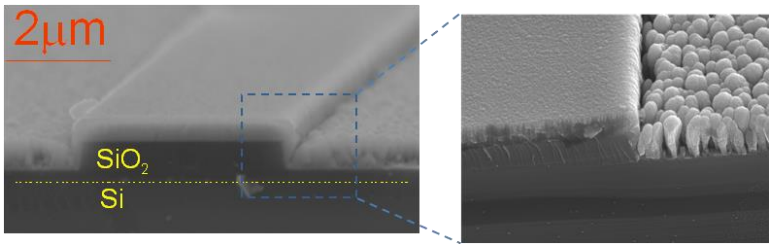

(a) (b)

Figure 4. (a) SEM image of the Er^{3+}/Yb^{3+} codoped BGO pedestal waveguide (b) zoom view.

The propagation losses decreased with increasing waveguide width[14] and a rapid increase in loss is observed for waveguide width smaller than 20 μm. Higher losses presented by smaller waveguides are due to the stronger interaction between the guided modes and waveguide sidewall roughness[15]. High losses of 7 dB/cm were also reported for Er^{3+} doped silicon-rich, silicon-oxide waveguide amplifier containing Si nanocrsytals[6]. Optical waveguides using Er-doped silica layers containing Si nanoclusters grown by reactive sputtering exhibited propagation losses of approximately 6 dB/cm at wavelength of 1310 nm[16]. We performed the near-field simulation, shown in Fig. 5(a), in order to estimate the transverse modes of the waveguides, considering a minimum width of 3 μm and a sidewall thickness of 250 μm. The results show that a 3 μm waveguide can support 4 transverse electric propagation modes, suggesting multimode guiding for λ = 1542nm (shown is only one mode: TE_{03}). The experimental result of the near-field profile for a 3 μm wide waveguide is shown in figure 5(b). The near-field profiles for the waveguides characterized in this work (100 μm wide waveguides) with and without Si nanostructures are shown in figures 5(c) and (d) respectively.

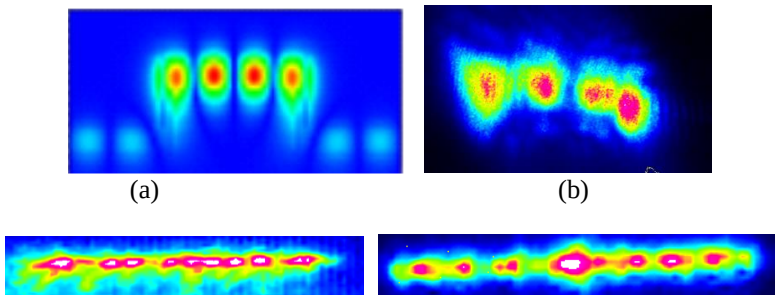

(a) (b)

(c) (d)

Figure 5. (a) Near field profile simulation for a 3 μm wide waveguide, showing TE03 mode at λ = 1542 nm. (b), (c) and (d) near field profiles captured for a 3 μm wide waveguide without Si, 100 μm wide waveguide with Si and 100 μm wide waveguide without Si, respectively.

During laser operation amplification of spontaneous emission (ASE) was observed in some waveguides containing Si, not noticed in waveguides without nanocrystals. Figures 6a and 6b show the spectra of two waveguides containing Si, with spontaneous and stimulated emission. The results show the strong influence of

the Si nanocrystals on the excitation of the RE ions. However, it also indicates that the fabrication methodology of the waveguides can be exploited to optimize the results related to the stimulated emission phenomena.

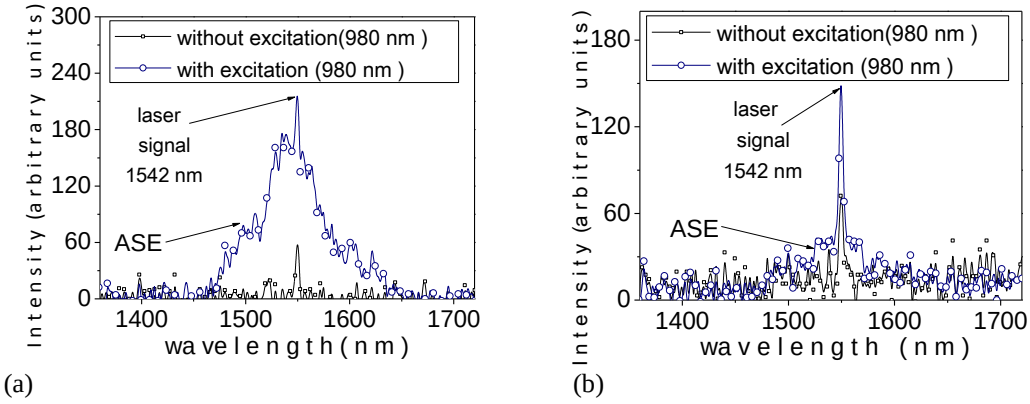

Figure 6. Photoluminescence spectra detected during gain measurements of the waveguides containing Si nanocrystals. (a) waveguide presenting a strong ASE. (b) waveguide with strong stimulated emission.

Figure 7 shows the results of the internal gain at 1542 nm of the Er^{3+}/Yb^{3+} codoped BGO pedestal waveguides with dimensions 100 µm x 1 cm (width x length) with and without Si nanocrystals as a function of pump power at 980 nm. At the maximum pump power of 60 mW an internal gain of 5.5 dB/cm and 3.5 dB/cm was measured for waveguides with and without Si, respectively.

It's important to notice that Si nanocrystals with diameter around 8 nm do not present quantum confinement and their direct energy bandgap does not differ much from the bandgap of bulk silicon (1.12eV)[17, 18]. At the filling fraction of Si NPs observed in our samples, an increase of the effective refractive index of the waveguides should be obtained. This enhancement of the refractive index must decrease the intrinsic losses of BGO waveguides associated to border defects and irregular morphology and enhance the guiding effect within the waveguides. In addition, Si nanostructures behave as a source of scattering, which could be linked to an increase of pump photon path length inside the waveguide and, therefore, to an increase of absorption and gain[24-28].

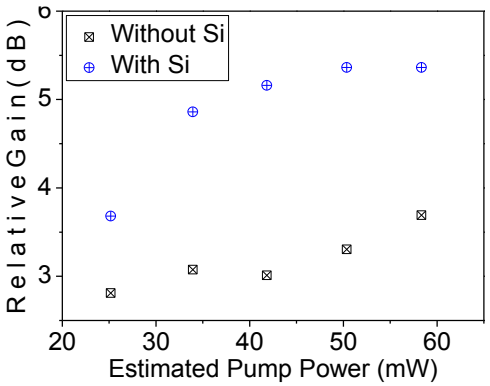

Figure 7. internal gain of Er^{3+}/Yb^{3+} codoped BGO pedestal waveguides (100 µm width) with and without silicon, under 980 excitation, as a function of the pump power.

4. CONCLUSIONS

This is the first observation of the influence of silicon nanocrystals in the amplification of the 1530 nm emission in Yb^{3+}/Er^{3+} codoped Bi_2O_3-GeO_2 pedestal waveguides. The present results show the possibility of producing silicon nanocrystals using the RF-sputtering technique followed by adequate heat treatment. The optical gain was enhanced by 50% and reached 5.5 dB/cm at 1530 nm. Large photoluminescence enhancement was observed in the visible and infrared regions in the presence of the silicon nanocrystals. These results open new possibilities for pedestal waveguides fabrication and their applications in integrated optics, such as nonlinear optical devices based on pedestal waveguides in codoped heavy metal oxide glasses containing metallic or semiconductor nanoparticles[19-23].

ACKNOWLEDGEMENTS

We would like to thank CNPq (grant 307989 2013-5), CAPES and FAPESP (grants 2017 10765-5 and 2016 02326-9). We also acknowledge the financial support from the National Institute of Photonics (INCT de Fotônica) supported by CNPq, the Nanotechnology National Laboratory (LNNano), CNPEM-Campinas/Brazil for the HR-TEM measurements and the Polytechnic School of USP.

REFERENCES

[1] Chen, T. and Liu, Y., [Semiconductor, Nanocrystals and Metal Nanoparticles: Physical Properties and Device Applications], Taylor & Francis Inc, (2016).
[2] de Araújo, C. B., da Silva, D. S., de Assumpção, T. A. A., Kassab, L. R. P., and da Silva, D. M., "Enhanced Optical Properties of Germanate and Tellurite Glasses Containing Metal or Semiconductor Nanoparticles," The Scientific World Journal 2013(385193), 1-13 (2013).
[3] de Assumpção, T. A. A., Kassab, L. R. P., Gomes, A. S. L., de Araújo C. B. and Wetter, N. U., " Influence of the heat treatment on the nucleation of silver nanoparticles in Tm^{3+} doped PbO-GeO_2 glasses," Appl Phys B 103, 165-169 (2011).
[4] Prasad, P. N., [Nanophotonics], Wiley (2004).
[5] Koshida, [Device Applications of Silicon Nanocrystals and Nanostructures. Series: Nanostructure Science and Technology], Springer (2009).
[6] Han, H. S., Seo, Y, S.and Shin, J. H., "Coefficient determination related to optical gain in erbium-doped silicon-rich silicon oxide waveguide amplifier," Appl. Phys. Lett. 81, 3720-3722 (2002).
[7] Kassab, L. R. P., Fukumoto, M. E., Cacho, V. D. D., Wetter, N. U. and Morimoto, N., I., "Spectroscopic properties of Yb^{3+} doped PbO–Bi_2O_3–Ga_2O_3 glasses for IR laser applications," Appl. Phys. Lett. 81, 3720-3722 (2002).
[8] Bonfim, F. A., Martinelli, J. R., Kassab, L. R. P., Wetter, N. U. and Neto, J. J., , "Effect of the ytterbium concentration on the upconversion luminescence of Yb^{3+}/Er^{3+} co-doped PbO–GeO_2–Ga_2O_3 glasses," J Non-Cryst. Solids 354, 4755-4759 (2008).
[9] da Silva, D. S., Naranjo, L. P., Kassab, L. R. P., de Araújo C. B., "Photoluminescence from germanate glasses containing silicon nanocrystals and erbium ions," Appl. Phys. B Lasers Opt. 106, 1015-1018 (2012).
[10] de Assumpção, T. A. A., da Silva, D. M., Cacho, V. D. D., Kassab, L. R. P., Alayo, M. I., "Production and characterization of Tm^{3+}/Yb^{3+} codoped waveguides based on PbO-GeO_2 thin films" J. Alloys Compd. 586, 368-372 (2014).
[11] Okamura, Y., Yoshinaka, S., Yamamoto, S., "Measuring mode propagation losses of integrated optical waveguides: a simple method," Appl. Opt. **22**, 3892-3894 (1983).
[12] Bomfim, F. A., da Silva, D. M., Kassab, L. R. P., de Assumpção T. A. A., Cacho, V. D. D., Alayo, M. I., "Advances on the fabrication process of Er^{3+}/Yb^{3+}: GeO_2–PbO pedestal waveguides for integrated photonics," Opt. Mater. 49, 196-200 (2015).
[13] Goodhew, P. J., Humphreys, J., Beanland, R., [Electron Microscopy and Analysis, 3ª ed] Taylor & Francis (2001).

[14] Poulton, C. G., Koos, C., Fuji, M., Pfang, A., Schimmel, T., Leuthold, J. and Freude, W., "Radiation modes and roughness loss in high index-contrast waveguides," Sel. Top. Quant. Electron. 12, 1306-1321 (2006).
[15] Tien, P. K., "Light Waves in Thin Films and Integrated Optics," Appl. Opt. 10, 2395-2413 (1971).
[16] Daldosso, A., Urios, D. N., Melchiorri, M., Pavesi, L., Gourbilleau, F., Carrada, M., Rizk, R., Garcia, C., Pellegrino, P., Garrido, B. and Cognolato, L., "Absorption cross section and signal enhancement in Er-doped Si nanocluster rib-loaded waveguides," Appl. Phys. Letters 86, 261103-1- 261103 -3 (2005).
[17] da Silva, D. S., de Assumpção, T. A. A., de Simone, G. B. C., Kassab, L. R. P. and de Araújo C. B., "Enhanced Er^{3+} photoluminescence in TeO_2–ZnO glass containing silicon nanocrystals," Appl. Phys. B Lasers Opt. 121, 117-121 (2015).
[18] Pavesi, L., Turan, R., [Silicon Nanocrystals: Fundamentals, Synthesis and Applications], Wiley (2010).
[19] De Assumpção, T. A. A., Da Silva, D. M., Camilo, M. E., Kassab, L. R. P., Gomes, A. S. L., De Araújo, C. B. and Wetter, N. U., "Frequency upconversion properties of Tm $^{3+}$ doped TeO 2-ZnO glasses containing silver nanoparticles," J. Alloys Compd. **536**, 504-506 SUPPL.1 (2012).
[20] Kassab, L. R. P., Courrol, L. C., Morais, A. S., Mendes, C. M. S. P., Tatumi, S. H., Wetter, N. U., Gomes, L. and Salvador, V. L. R., "Spectroscopic properties of lead fluoroborate and heavy metal oxide glasses doped with Yb^{3+}," J. Non. Cryst. Solids **304**,233-237 (2002).
[21] De Assumpção, T. A. A., Kassab, L. R. P., Gomes, A. S. L., De Araújo, C. B. and Wetter, N. U., "Influence of the heat treatment on the nucleation of silver nanoparticles in Tm3+ doped PbO-GeO2 glasses," Appl. Phys. B Lasers Opt. **103**(1), 165-169 (2011).
[22] Bomfim, F. A., Martinelli, J. R., Kassab, L. R. P., Wetter, N. U. and Neto, J. J., "Effect of the ytterbium concentration on the upconversion luminescence of Yb3+/Er3+ co-doped PbO-GeO2-Ga2O3 glasses," J. Non. Cryst. Solids **354**, 4755-4759 (2008).
[23] Kassab, L. R. P., Courrol, L. C., Morais, A. S., Tatumi, S. H., Wetter, N. U. and Gomes, L., "Spectroscopic properties of lead fluoroborate glasses codoped with Er $^{3+}$ and Yb^{3+}," J. Opt. Soc. Am. B Opt. Phys. **19**(12), 2921-2926 (2002).
[24] Jimenez-Villar, E., Mestre, V., de Oliveira, P. C. and de Sá, G. F., "Novel core–shell (TiO2@Silica) nanoparticles for scattering medium in a random laser: higher efficiency, lower laser threshold and lower photodegradation," Nanoscale **5**(24), 12512 (2013).
[25] Jimenez-Villar, E., Mestre, V., de Oliveira, P. C., Faustino, W. M., Silva, D. S. and de Sá, G. F., "TiO 2 @Silica nanoparticles in a random laser: Strong relationship of silica shell thickness on scattering medium properties and random laser performance," Appl. Phys. Lett. **104**(8), 81909 (2014).
[26] Jimenez-Villar, E., da Silva, I. F., Mestre, V., de Oliveira, P. C., Faustino, W. M. and de Sá, G. F., "Anderson localization of light in a colloidal suspension (TiO 2 @silica)," Nanoscale **8**(21), 10938–10946 (2016).
[27] Jiménez-Villar, E., da Silva, I. F., Mestre, V., Wetter, N. U., Lopez, C., de Oliveira, P. C., Faustino, W. M. and de Sá, G. F., "Random Lasing at Localization Transition in a Colloidal Suspension (TiO 2 @Silica)," ACS Omega **2**(6), 2415–2421 (2017).
[28] Wetter, N. U., Giehl, J. M., Butzbach, F., Anacleto, D. and Jiménez-Villar, E., "Polydispersed Powders (Nd 3+ :YVO 4) for Ultra Efficient Random Lasers," Part. Part. Syst. Charact., 1700335 (2017).